Mon. Not. R. Astron. Soc. **332,** 193–198 (2002)

Principal-component analysis of the cosmic microwave background anisotropies: revealing the tensor degeneracy

G. Efstathiou[1,2]★

[1]*Institute of Astronomy, Madingley Road, Cambridge CB3 0HA*
[2]*Theoretical Astrophysics, Caltech, Pasadena, CA 91125, USA*

Accepted 2001 December 18. Received 2001 December 17; in original form 2001 September 14

ABSTRACT

A principal-component analysis of cosmic microwave background (CMB) anisotropy measurements is used to investigate degeneracies among cosmological parameters. The results show that a degeneracy with tensor modes – the 'tensor degeneracy' – dominates uncertainties in estimates of the baryon and cold dark matter densities, $\omega_b = \Omega_b h^2$, $\omega_c = \Omega_c h^2$,[1] from an analysis of CMB anisotropies alone. The principal-component analysis agrees well with a maximum-likelihood analysis of the observations, identifying the main degeneracy directions and providing an impression of the effective dimensionality of the parameter space.

Key words: cosmic microwave background – cosmology: miscellaneous.

1 INTRODUCTION

Since the discovery of cosmic microwave background (CMB) anisotropies by the *COBE* team (Smoot et al. 1992) there has been rapid progress on the observational front, culminating with the publication earlier this year of evidence for multiple acoustic peaks in the CMB power spectrum (Lee et al. 2001; Halverson et al. 2002; Netterfield et al. 2002). It has long been known that accurate measurements of the CMB anisotropies can be used to estimate parameters characterizing the primordial fluctuations, the geometry of the Universe and its matter content (e.g. Jungman et al. 1996; Bond, Efstathiou & Tegmark 1997; Zaldarriaga, Spergel & Seljak 1997). In fact, the most recent measurements paint a gratifyingly consistent picture compatible with the simplest models of inflation (i.e. a spatially flat universe with scale-invariant adiabatic fluctuations). Furthermore, the derived value of the baryon density ω_b appears to be consistent with the value $\omega_b = 0.020 \pm 0.002$ inferred from primordial nucleosynthesis and deuterium abundance measurements from quasar absorption-line spectra (Burles, Nollett & Turner 2001, and references therein).

It has also long been known that there are significant degeneracies amongst cosmological parameters estimated from CMB anisotropies, i.e. parameter combinations exist that produce nearly identical CMB power spectra (Bond et al. 1994; Efstathiou & Bond 1999, hereafter EB99). The best known is the *geometrical degeneracy* between the matter and vacuum energy densities, Ω_m and Ω_Λ, and the curvature $\Omega_k = 1 - \Omega_m - \Omega_\Lambda$. This degeneracy is almost exact and precludes reliable estimates of either Ω_Λ or the Hubble parameter h from measurements of the CMB anisotropies alone. The existence of parameter degeneracies means that the best-fitting parameters and their errors can be extremely sensitive to the chosen parameter set (e.g. whether the Universe is assumed to be spatially flat) and to adopted 'prior distributions' (e.g. observational constraints on the Hubble constant). This complicates the interpretation of CMB anisotropy parameter studies and the intercomparison of limits determined by different authors.

Tensor modes have been considered in a number of earlier analyses of CMB anisotropies (see, e.g., Tegmark 1999; Melchiorri et al. 1999; Zibin, Scott & White 1999; Hannestad, Hansen & Villante 2001; Kinney, Melchiorri & Riotto 2001; Tegmark, Zaldarriaga & Hamilton 2001). However, most of the analyses of the recent CMB data have ignored a tensor component (see, for example, Lange et al. 2001; Jaffe et al. 2001; Stompor et al. 2001; de Bernardis et al. 2002; Pryke et al. 2002). This special case is certainly interesting because a wide class of inflationary models predict a negligible contribution from tensor modes. Indeed, it has been argued persuasively that the absence of tensor modes is generic to any model in which the inflaton potential is related to the Higgs sector of a grand unified theory (Lyth 1997).

However, so little is known about inflation (if indeed inflation occurred) that it may be dangerous to neglect a tensor mode, particularly if some cosmological parameters of interest are sensitive to tensor modes. In fact, in single-field inflation models the relative amplitudes of the tensor and scalar tensor modes (r) and their spectral indices (n_t and n_s) are related to the inflaton potential and its first two derivatives (e.g. see Hoffman & Turner 2001 for a recent discussion). In this class of model the relation between n_s and n_t is model-dependent, while the relation between n_t and r depends only on the validity of the slow-roll approximation. However, even the latter relation can be violated in multifield inflationary models. These relations may also be

★E-mail: gpe@ast.cam.ac.uk

[1] Here h is Hubble's constant H_0 in units of $100\,\mathrm{km\,s^{-1}\,Mpc^{-1}}$.

violated in some superstring-inspired models (see, e.g., Lidsey, Wands & Copeland 2000 and references therein). Examples of the latter include the pre-big-bang model of Veneziano and collaborators (e.g. Buonnono, Damour & Veneziano 1999), which it is argued can lead to 'blue' scalar spectral indices ($n_s > 1$), and the ekpyrotic scenario (Khoury et al. 2001), which produces a strongly blue tensor mode spectrum.

The point of view taken in this paper is to define a minimal parameter set on the assumption that the primordial fluctuations are Gaussian, adiabatic and featureless (i.e. defined by power-law spectral indices). Thus the minimal model is specified by nine parameters: four parameters specifying the amplitudes and spectral indices of scalar and tensor components ($\bar{Q}$, r_{10}, n_s and n_t, see Section 2 for more precise definitions), four parameters defining the matter content and curvature of the Universe (ω_b, ω_c, Ω_Λ, Ω_k) and a single parameter τ_{opt} quantifying the optical depth to Thomson scattering since the Universe was reionized. However, as pointed out by EB99, including a tensor component with no assumed constraints between the parameters n_s, n_t and r_{10} introduces a new major degeneracy between cosmological parameters that we will call the *tensor degeneracy* in this paper. This degeneracy has a dramatic effect on the permitted ranges of some parameters, in particular the baryon and cold dark matter densities ω_b and ω_c. The minimal model with nine parameters suffices to demonstrate the main parameter degeneracies. Adding additional parameters, for example, allowing massive neutrinos will make the degeneracies worse, though comparison of the results of this paper with those of Wang, Tegmark & Zaldarriaga (2002) shows that massive neutrinos have little effect on the results described in Section 2.

In fact, it is easy to construct models with even more severe parameter degeneracies than those described here. For example, the parameter degeneracies are made worse in hybrid models including adiabatic perturbations and cosmic defects (e.g. Bouchet et al. 2000) and/or isocurvature perturbations (Bucher, Moodley & Turok 2001). For general isocurvature and adiabatic perturbations, Bucher et al. show that accurate estimates of the cosmological parameters, including the cosmic densities ω_b and ω_c, require extremely accurate CMB polarization measurements in addition to temperature anisotropy measurements.

One approach to analysing parameter degeneracies is to apply brute-force maximum-likelihood analysis to a large parameter set (see, e.g., Wang et al. 2002; Efstathiou et al. 2002 and references therein). Here we show that the observational data has now improved to the point that a simple principal-component analysis of the Fisher matrix defined by the data identifies the major degeneracy directions (geometrical and tensor) and provides a useful first approximation to the likelihood function. Using the principal components it is easy to analyse the correlations between physical parameters introduced by the tensor degeneracy and to assess the effects of introducing external (non-CMB) constraints on the parameters.

2 PRINCIPAL-COMPONENT ANALYSIS

We use the compilation of band power estimates ΔT_B^2 and their covariance matrix $C_{BB'}$ computed by Wang et al. (2002, hereafter WTZ02) from 105 CMB anisotropy measurements. These band power estimates include a model for calibration and beam errors (see WTZ02 for further details). Each band power estimate is related to the power spectrum C_ℓ of the CMB anisotropies by

$$\Delta T_B^2 = \frac{T_0^2}{2\pi}\sum_\ell \ell(\ell+1)C_\ell W_B(\ell), \tag{1}$$

where W_B is the window function for each band power (also computed by WTZ02). These band-power estimates are plotted in Fig. 1. Also plotted in this figure is a fiducial model[2] with the following parameters: $\omega_b = 0.020$, $\omega_c = 0.13$, $h = 0.7$ ($\Omega_b = 0.04$, $\Omega_c = 0.26$), $\Omega_k = 0$, $\tau_{opt} = 0.1$, $n_s = 1$, $n_t = 0$, $r_{10} = 0.2$. These parameters provide an extremely good fit to the observations and are very close to the concordance values determined by WTZ02 and the author from a full likelihood analysis. The addition of a small tensor component has little effect on the fit shown in Fig. 1, but is introduced to regularize the Fisher matrix of equation (2).

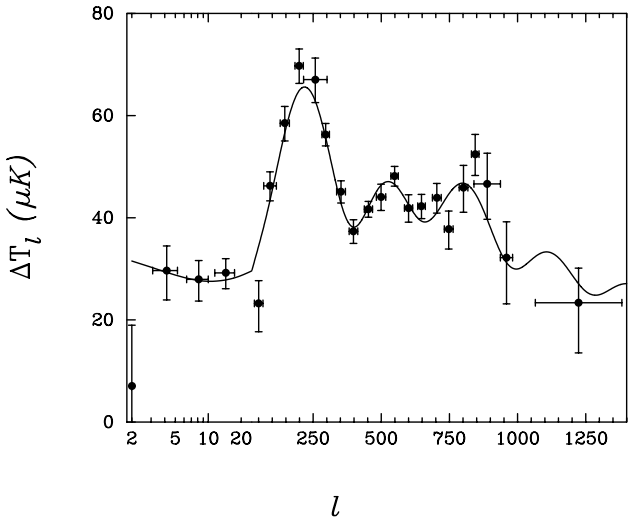

Figure 1. The points show band-averaged observational estimates of the CMB power spectrum from WTZ02 plotted against multipole index using a log-linear abscissa. The error bars show $\pm 1\sigma$ errors. The line shows the CMB power spectrum for the fiducial inflationary model discussed in the text.

Given the covariance matrix of the observations, we can form the Fisher matrix for the (mean subtracted) parameter set $\{s_i\}$:

$$F_{ij} = \sum_{BB'} C^{-1}_{BB'} \frac{\partial \Delta T_B^2}{\partial s_i}\frac{\partial \Delta T_{B'}^2}{\partial s_j}. \tag{2}$$

In defining the parameter set s_i, we use ln ω_b and ln ω_c rather than ω_b and ω_c and $\Omega_D = \Omega_k - 0.286\Omega_\Lambda$ rather than Ω_k. The latter expresses the geometrical degeneracy (see EB99), since if all parameters other than Ω_k and Ω_Λ are held fixed, the condition $\delta\Omega_D = 0$ preserves the positions of the acoustic peaks for small variations of the parameters about those of the fiducial model. The normalization parameter $\bar{Q}$ is defined following EB99 so that $\bar{Q}^2$ is the mean band power $[\sum_{\ell<1500}\ell(\ell+1)C_\ell]$ of a model relative to that of the fiducial model plotted in Fig. 1. With this definition, $\bar{Q}$ is observationally well constrained and is largely decoupled from variations in cosmology and the optical depth τ_{opt} (unlike measures of the amplitude related to low multipoles). The tensor-to-scalar ratio r_{10} is defined so that $C_{10}^T = r_{10}C_{10}^S$. With these definitions, we can compute the Fisher matrix (2) from derivatives of the power

[2] The CMB power spectra in this paper were computed using the CMBFAST code of Seljak & Zaldarriaga (1996).

Table 1. Principal components for data of Fig. 1.

	$\lambda_i^{-1/2}$	$\ln \omega_b$	$\ln \omega_c$	n_s	$\bar{Q}$
X_1	8.4923E−03	8.0062E−02	−1.8131E−01	2.0836E−02	−1.5648E−01
X_2	1.6231E−02	2.9071E−02	−3.1679E−02	−3.7260E−01	9.0306E−01
X_3	3.1626E−02	−1.5949E−01	−1.0387E−01	8.0645E−01	3.9347E−01
X_4	7.1340E−02	−7.3973E−01	1.7199E−01	1.7869E−01	−1.1711E−02
X_5	1.3033E−01	5.4011E−01	6.8276E−01	3.2525E−01	7.0219E−02
X_6	2.8274E−01	−2.1034E−01	4.2130E−01	−1.2216E−01	−9.8231E−03
X_7	8.9800E−01	2.1023E−01	−3.8577E−01	1.4257E−01	−1.7712E−03
X_8	1.5724E+00	1.9488E−01	−3.5449E−01	1.8691E−01	3.5187E−03
X_9	3.8197E+00	−4.4314E−02	8.7287E−02	−4.9695E−02	−1.3832E−03
$\langle s_i^2 \rangle^{1/2}$		0.41	0.75	0.38	0.023
	τ_{opt}	Ω_Λ	Ω_D	n_t	r_{10}
X_1	−6.8989E−03	−3.0498E−03	9.6731E−01	3.1160E−03	−6.4147E−03
X_2	1.0592E−01	6.3355E−02	1.4733E−01	−4.5002E−02	6.9623E−02
X_3	−2.9357E−01	−1.8037E−01	3.5921E−02	1.1322E−01	−1.6053E−01
X_4	4.2868E−01	3.4928E−01	9.3853E−02	−1.7909E−01	2.1096E−01
X_5	2.4081E−01	2.1371E−01	9.0979E−02	−1.0073E−01	9.6515E−02
X_6	−4.0134E−01	−5.1452E−01	9.6988E−02	−9.6036E−02	5.6463E−01
X_7	−3.3061E−01	4.5135E−01	−8.9152E−02	−4.5136E−01	5.1182E−01
X_8	5.7374E−01	−3.6421E−01	−8.0544E−02	2.6539E−01	5.1250E−01
X_9	−2.4747E−01	4.4122E−01	1.9666E−02	8.1212E−01	2.6851E−01
$\langle s_i^2 \rangle^{1/2}$	1.3	1.8	0.17	3.1	1.4

spectra C_ℓ^S and C_ℓ^T, as in standard analyses of parameter forecasting (Jungman et al. 1996; Bond et al. 1997). Alternatively, we could compute the Hessian matrix by estimating second derivatives of the likelihood function around the maximum-likelihood value either directly or by summing over first and second derivatives of ΔT_B^2. In most situations using either the Fisher or Hessian matrices should give very similar results, and in fact, the second derivatives of ΔT_B^2 are often ignored in order to stabilize the numerical evaluation of the Hessian (see, e.g., Press et al. 1992).

Having computed the Fisher matrix, we diagonalize it,

$$\mathbf{F} = \mathbf{U}\mathbf{\Lambda}\mathbf{U}^T, \qquad \mathbf{\Lambda} = \mathrm{diag}(\lambda_1, \lambda_2, \ldots, \lambda_N). \tag{3}$$

The matrix $\mathbf{U}$ defines a set of principal components, $\mathbf{X}$, i.e. orthogonal linear combinations of the original parameters,

$$\mathbf{X} = \mathbf{U}^T\mathbf{s}, \tag{4}$$

such that the variance of the component X_i is equal to $1/\lambda_i$. See BE99 for an application of principal-component analysis to the *MAP* and *Planck* satellites.[3]

The eigenvalues and components of $\mathbf{U}^T$ for our chosen set of variables and fiducial model are listed in Table 1. The principal components have been ordered by their expected variance so that X_1 is the best-determined parameter and X_9 is the worst. The last line in the table lists the predicted variances of the parameters s_i, $[\sqrt{(F_{ii}^{-1})}]$. As can be seen from Table 1, the present data can be used to constrain three parameter combinations well and three extremely poorly, with the remaining being constrained at intermediate levels of accuracy. The best- and worst-determined principal components have a straightforward interpretation. X_1 has a high weight from Ω_D, and so, in effect, measures the positions of the acoustic peaks; X_2 has a high weight from the overall amplitude of the spectrum $\bar{Q}$; X_3 has high weights from the scalar spectral index n_s and τ_{opt} and provides a measure of the shape of the fluctuation spectrum. The component X_9 accounts for almost all of the variance of Ω_Λ, n_t and r_{10}, and describes the geometrical degeneracy and the extremely poor constraints that the present data place on tensor modes. The component X_8 describes the tensor degeneracy and accounts for almost all of the variance of the parameters $\ln \omega_b$, $\ln \omega_c$, n_s and Ω_D. Together, the components X_9 and X_8 account for almost all of the variance of all of the parameters with the exception of the amplitude $\bar{Q}$.

The principal-component analysis therefore suggests that acceptable models lie on a plane within the nine-dimensional parameter space. This is illustrated in Fig. 2(a) which shows likelihood contours in projections chosen to illustrate the geometrical and tensor degeneracies. The upper panels show the geometrical degeneracy in the parameter pairs $\Omega_\Lambda - \Omega_k$ and $h - \Omega_\Lambda$. The dashed lines show the degeneracy directions defined by the component X_9. The solid line in the $\Omega_\Lambda - \Omega_k$ plane shows the constraint $\delta\Omega_D = 0$. The solid line in the $h - \Omega_\Lambda$ plane is computed from the constraint equation

$$h = \frac{(\omega_b + \omega_c)^{1/2}}{(1 - \Omega_k - \Omega_\Lambda)^{1/2}} = \frac{(\omega_b + \omega_c)^{1/2}}{\left(1 - \Omega_D - \frac{4.5}{3.5}\Omega_\Lambda\right)^{1/2}}, \tag{5}$$

with ω_b, ω_c and Ω_D set to the values of the target model. The dotted lines in the lower two panels show the degeneracy directions defined by the component X_8.

The Fisher matrix and the associated principal-component analysis is approximate and it is not obvious a priori how well they describe degeneracies especially for parameter values that are quite a long way from those of the target model. Fig. 2(b) shows the analogous contours computed from a full likelihood analysis of the data of Fig. 1 [see the companion paper of Efstathiou et al. (2002) for a detailed discussion]. The agreement is surprisingly good. The general directions of the geometrical and tensor degeneracies follow those of the Fisher matrix analysis. There are some differences, however. The low-order CMB multipoles offer some

[3] Descriptions of these satellites can be found on the following web pages: http://astro.estec.esa.nl/SA-general/Projects/Planck and http://map.gsfc.nasa.gov

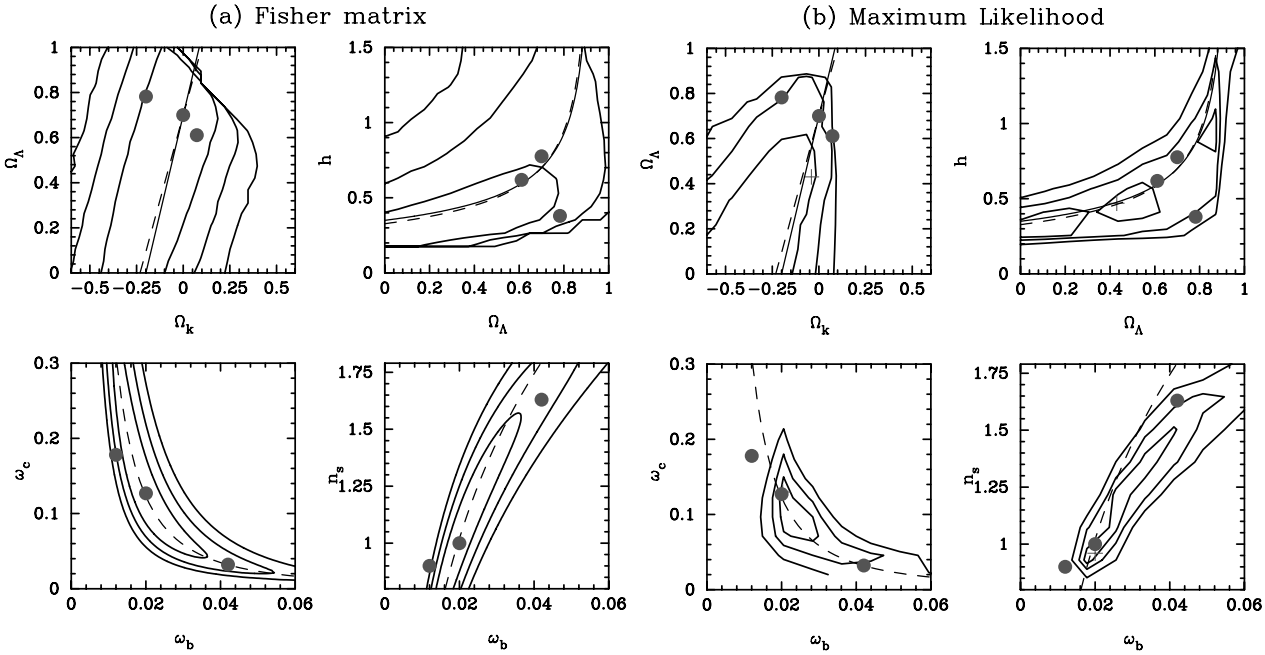

Figure 2. Various projections of the likelihood functions chosen to illustrate the geometrical and tensor degeneracy. One, two and three-sigma likelihood contours are plotted in each panel. The panels to the left were computed from the Fisher matrix (equation 2) and the panels to the right show 'pseudo-marginalized' contours computed from a full likelihood analysis of the data described by Efstathiou et al. (2002). The solid lines in the upper panel show the approximate locus of the geometrical degeneracy computed from the constraint $\Omega_D =$ constant and from the constraint equation (5). The dashed lines in the upper and lower panels show the degeneracy directions defined by the component X_9 and X_8, respectively. The filled circles show the parameters of the nearly degenerate models plotted in Fig. 3. The crosses in (b) show the positions of the peaks in the likelihood function.

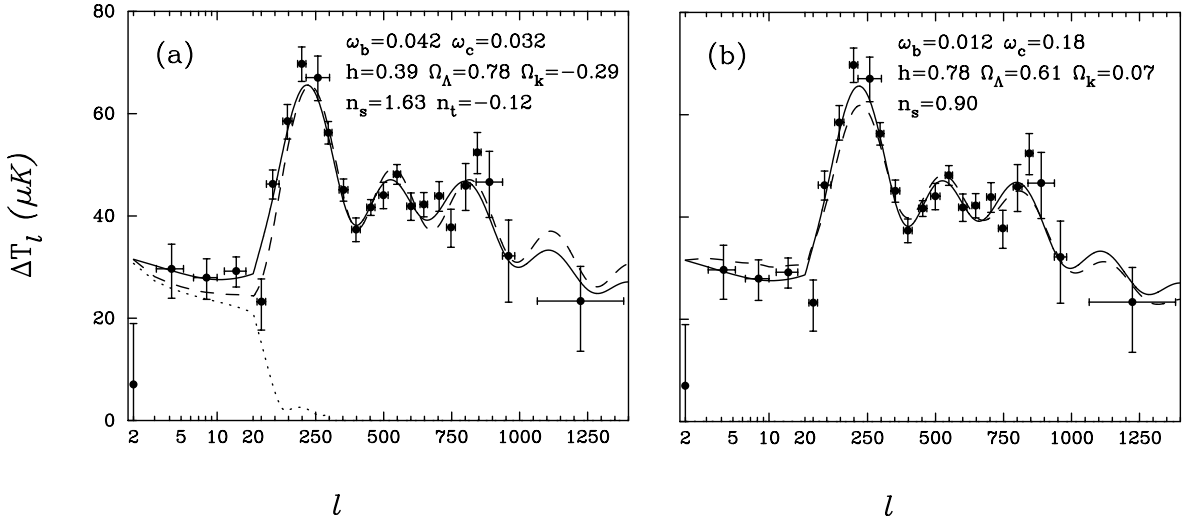

Figure 3. The data and fiducial model (solid line) of Fig. 1. The dashed lines show CMB power spectra for nearly degenerate models with a high baryon density (a) and a low baryon density (Fig. 3b) chosen to lie along the direction of the tensor degeneracy. The dotted line in (a) shows the contribution of the tensor component. The low model with low baryon density in (b) has a negligible contribution from tensor modes.

discrimination of models with high values of Ω_Λ via the integrated Sachs–Wolfe effect (see EB99), thus models with $\Omega_\Lambda \gtrsim 0.88$ are excluded by the data. The maximum-likelihood analysis shows that the tensor degeneracy allows high values of ω_b but that the likelihood function falls sharply for $\omega_b \lesssim 0.018$ (interestingly only just below the value favoured from primordial nucleosynthesis deuterium constraints).

The three filled circles in Fig. 2 show the parameter values for the target model and for two nearly degenerate models with extreme values of ω_b chosen to lie along the tensor degeneracy direction. (The device used here, of varying low-order principal components to produce degenerate pairs of models, was used by EB99 to investigate parameter degeneracies for the *MAP* and *Planck* satellites.) One model has $\omega_b = 0.042$ and the other has $\omega_b = 0.012$. The models were chosen intentionally to have similar values of Ω_Λ, consequently the high baryon density model has a low value of h, which one might argue is incompatible with independent measurements of the Hubble constant (Freedman et al. 2001). However, our purpose here is to show how the constraints on ω_b derived from CMB anisotropies *alone* are weakened when tensor modes are included. The high and low baryon density models are compared with the data and the fiducial model in Fig. 3.

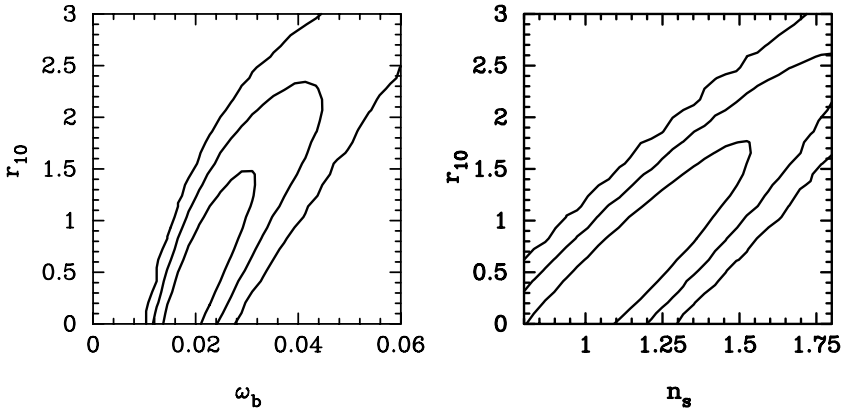

Figure 4. Fisher matrix likelihood contours (at one, two and three-sigma levels) in the $r_{10}-\omega_b$ and $r_{10}-n_s$ planes.

Despite the very different parameter values, the models produce almost identical CMB power spectra by construction. The exact likelihood analysis (Fig. 2b) shows that the model with high baryon density is compatible with the data at approximately the 2σ level. The low baryon density model is formally excluded by the data at a high level of significance ($>3\sigma$) because it fails to match the height of the first acoustic peak. This is a characteristic feature of models with a low baryon density. Nevertheless, the diagram is interesting because it shows that the lower limits on ω_b are extremely sensitive to any residual systematic errors that might affect the peak heights (see, e.g., de Bernardis et al. 2002, fig. 1).

Any model with a high baryon density $\omega_b \gtrsim 0.03$ that provides an acceptable fit to the CMB data must necessarily be tensor-dominated at low multipoles ($r_{10} \gtrsim 1$) and have a strongly tilted scalar fluctuation spectrum. This is illustrated in Fig. 4, which shows the Fisher matrix likelihood contours in the $r_{10}-\omega_b$ and $r_{10}-n_s$ planes. However, this diagram shows that the converse is not true; tight independent constraints on ω_b or n_s do not lead to tight constraints on r_{10}. This is consistent with the full likelihood analysis presented by Efstathiou et al. (2002), including constraints from the 2dF Galaxy Redshift Survey and from big-bang nucleosynthesis.

3 DISCUSSION

The reader might question the usefulness of the results presented in the previous section. First, the principal-component analysis provides only an approximate description of the parameter degeneracies, whereas they emerge precisely from a brute-force maximum-likelihood analysis. Secondly, models at the extreme ends of the ranges allowed by the tensor degeneracy have unusual parameters (for example, the model with $\omega_b = 0.042$ in Fig. 3(b) has a low Hubble constant and a high value of the scalar spectral index) and so are surely excluded by other observational constraints. We discuss each of these points in turn.

(i) *Effective dimensionality.* The main use of the principal-component analysis is to assess the effective dimensionality of the space of acceptable models within the multidimensional space defined by the physical parameters s_i and to assess whether this effective dimensionality is sensitive to changes of the parameter set. For example, let us assume that we are interested in the values of the parameters ω_b and ω_c. The principal-component analysis tells us that most of the variance of these parameters is contributed by only two poorly constrained principal components. The values of these parameters are therefore affected by major parameter degeneracies which can only be removed by imposing external constraints or by performing a fundamentally different type of CMB experiment. For example, the effects of the tensor degeneracy on ω_b and ω_c can be broken by extending the CMB measurements to much higher multipoles (see EB99) and/or by setting limits on a tensor component from an analysis of a B-type polarization pattern in the CMB (see, e.g., Kamionkowski & Jaffe 2000, and references therein).

(ii) *Complementary information.* CMB parameter degeneracies can be broken by invoking complementary information. A well-known example is the combination of type Ia supernovae measurements with the CMB to break the geometrical degeneracy (see, e.g., de Bernardis et al. 2002 for a recent analysis). WTZ02 break the tensor degeneracy by combining the CMB data with a number of constraints, including estimates of the power spectrum on small scales from observations of the Lyα forest (Croft et al. 2002) and limits on the Hubble constant from the *HST* Hubble Key Project (Freedman et al. 2001). The problem here is that it becomes progressively more difficult to assess whether parameter values are affected by systematic errors as more external constraints are applied, particularly if the external constraints involve complex observations and assumptions. (For example, how can we test empirically whether density fluctuations in the intergalactic medium as traced by the Lyα forest match those of the dark matter?). Even if the parameter values are shown to remain consistent as external constraints are applied, there is no guarantee that the final combined likelihood distribution will be accurate. Ideally, we would like to apply as small a number of external constraints as possible using data sets with well-controlled errors. The Fisher matrix analysis of the previous section offers a guide as to which external constraints will be most effective at breaking degeneracies. The effects of external constraints can easily be assessed using the Fisher matrix: let P_{ij} be the covariance matrix of the parameters s_i from external constraints, then the covariance matrix after combining with the CMB is

$$C_{ij} = (F_{ij} + P_{ij}^{-1})^{-1}. \quad (6)$$

As mentioned in Section 2, the models plotted in Fig. 3 were chosen by construction to have similar values of Ω_Λ, so it is clear that combining the CMB results with constraints on Ω_Λ from type Ia supernovae observations will have little effect on the parameters ω_b and ω_c. Constraints on the Hubble constant will be more effective in narrowing the range of allowed values of ω_b and ω_c. However, from Fig. 2 we can see that the tensor degeneracy exhibits a strong correlation between ω_b, ω_c and the scalar spectral

index n_s. Even a relatively poor constraint on the scalar spectral index will lead to a sharp tightening of the ω_b and ω_c error contours. [A constraint Δn_s on the spectral index will narrow the error on the baryon density to $\Delta \ln \omega_b \approx (U_{18}/U_{38})\Delta n_s$, i.e. $\Delta \ln \omega_b \approx 1.04 \Delta n_s$.] This suggests that the recent estimates of the galaxy power spectrum from the 2dF Galaxy Redshift Survey (Percival et al. 2001) will be highly effective at breaking the tensor degeneracy, leading to tight constraints on the matter content of the Universe. This is borne out by a detailed analysis presented in a companion paper (Efstathiou et al. 2002).

ACKNOWLEDGMENTS

I thank Caltech for the award of a Moore Scholarship. I thank Andrew Liddle for discussions of inflationary models and various members of the 2dF Galaxy Survey team and a referee for their comments on an earlier draft.

REFERENCES

Bond J. R., Crittenden R., Davis R. L., Efstathiou G., Steinhardt P. J., 1994, Phys. Rev. Lett., 72, 13
Bond J. R., Efstathiou G., Tegmark M., 1997, MNRAS, 291, L33
Bouchet F. R., Peter P., Riazuelo A., Sakellariadou M., 2001, Phys. Rev. D, 65, 021301
Bucher M., Moodley K., Turok N., 2001, Phys. Rev. Lett., 87, 1301
Buonnano A., Damour T., Veneziano G., 1999, Nucl. Phys. B, 543, 275
Burles S., Nollett K. M., Turner M. S., 2001, ApJ, 552, L1
Croft R. A. C., Weinberg D. H., Bolte M., Burles S., Hernquist L., Katz K., Kirkman D., Tytler D., 2002, ApJ, in press (astro-ph/0012324)
de Barnardis et al., 2002, ApJ, 564, 559
Efstathiou G., Bond J. R., 1999, MNRAS, 304, 75 (EB99)
Efstathiou G. et al., 2002, MNRAS, 330, L29
Freedman W. L. et al., 2001, ApJ, 553, 47
Halverston N. W. et al., 2002, astro-ph/0104489
Hannestad S., Hansen S. H., Villante F. L., 2001, Astropart. Phys., 16, 137
Hoffman M. B., Turner M. S., 2001, Phys. Rev. D, 64, 023506
Jaffe A. H. et al., 2001, Phys. Rev. Lett., 86, 3475
Jungman G., Kamionkowski M., Kosowsky A., Spergel D. N., 1996, Phys. Rev. D, 54, 1332
Kamionkowski M., Jaffe A. H., 2001, Int. J. Mod. Phys., A1651A
Khoury J., Ovrut B. A., Steinhardt P. J., Turok N., 2001, Phys. Rev. D, 123522
Kinney W. H., Melchiorri A., Riotto A., 2001, Phys. Rev. D, 63, 023505
Lange A. E. et al., 2001, Phys. Rev. D, 63, 042001
Lee A. T. et al., 2001, ApJ, 561, L1
Lidsey J. E., Wands D., Copeland E. J., 2000, Phys. Rev., 337, 343
Lyth D. H., 1997, Phys. Rev. Lett., 78, 1861
Melchiorri A., Sazhin M. V., Shulga V. V., Vittorio N., 1999, ApJ, 518, 562
Netterfield C. B. et al., 2002, astro-ph/0104460
Percival W. J. et al., 2001, MNRAS, 327, 1297
Press W. H., Teukolsky S. A., Vetterling W. T., Flannery B. P., 1992, Numerical Recipes. Cambridge Univ. Press, Cambridge
Pryke C., Halverson N. W., Leitch E. M., Kovac J., Carlstrom J. E., Holzapfel W. L., Dragovan M., 2002, ApJ, submitted (astro-ph/0104490)
Seljak U., Zaldarriaga M., 1996, ApJ, 469, 437
Smoot G. F. et al., 1992, ApJ, 396, L1
Stompor R. et al., 2001, ApJ, 561, L7
Tegmark M., 1999, ApJ, 514, L69
Tegmark M., Zaldarriaga M., Hamilton A. J. S., 2001, Phys. Rev. D, 63, 043007
Wang X., Tegmark M., Zaldarriaga M., 2002, Phys. Rev. D, in press (astro-ph/0105091) (WTZ01)
Zaldarriaga M., Spergel D. N., Seljak U., 1997, ApJ, 488, 1
Zibin J. P., Scott D., White M., 1999, Phys. Rev. D, 60, 123513

This paper has been typeset from a TEX/LATEX file prepared by the author.